RSC Advances

ROYAL SOCIETY OF CHEMISTRY

PAPER

View Article Online
View Journal | View Issue

Check for updates

Cite this: *RSC Adv.*, 2020, **10**, 42564

Reaction induced robust Pd_xBi_y/SiC catalyst for the gas phase oxidation of monopolistic alcohols†

Pengwei Wang,* Lijun Xu, Jianming Zhu, Kunqi Gao, Yan Zhang and Jifen Wang*

Received 14th September 2020
Accepted 13th November 2020

DOI: 10.1039/d0ra07859j

rsc.li/rsc-advances

Reaction induced Pd_xBi_y/SiC catalysts exhibit excellent catalytic activity (92% conversion of benzyl alcohol and 98% selectivity of benzyl aldehyde) and stability (time on stream of 200 h) in the gas phase oxidation of alcohols at a low temperature of 240 °C due to the formation of $Pd^0–Bi_2O_3$ species. TEM indicates that the agglomeration of the 5.8 nm nanoparticles is inhibited under the reaction conditions. The transformation from inactive $PdO–Bi_2O_3$ to active $Pd^0–Bi_2O_3$ under the reaction conditions is confirmed elaborately by XRD and XPS.

1. Introduction

Alcohol oxidation reaction is widely investigated in both laboratories and industrial applications due to the importance of its valuable products such as aldehydes and ketones, which are widely used in dyestuffs, polymer precursors, and pharmaceutical and agrochemical industries.[1–3] Traditionally, stoichiometric oxidants such as dichromate or permanganate are used in the liquid phase oxidation but are toxic and expensive, which could not meet the development of green chemistry. Hence, there is a need of shifting from methods based on the toxic and inorganic oxidants to greener and more atom efficient methods which adopt molecular oxygen as oxidant.[4–6]

Considering that lots of noble metal catalysts have been used in the oxidation of alcohols using O_2 as oxidant, Pd based catalysts have attracted much attention for its simple preparation method and excellent catalytic activity.[4] However, some problems still impede its industrial applications. For example, the formation process of active phase is investigated elaborately for Pd/SBA-15, but the agglomeration of the nanoparticles and low efficiency are inevitable.[7] Pd/Al_2O_3 is reported by Li *et al.*, however, the reduction of active PdO to inactive Pd^0 in the reaction conditions contributes to the deactivation of the catalyst.[8,9] Sulfur doped SBA-15 supported Pd exhibits excellent catalytic activity, however, the unstability of the amphorous Pd is adverse in industrial applications.[2] Novel highly stable and anti-sintered large size Pd/TiO_2 for the oxidation of benzyl alcohol has been reported, but the conversion of benzyl alcohol is lower than 50%.[3]

To improve the catalytic activity of Pd catalyst, bimetal Pd based catalysts in alcohol oxidation reaction have attracted increasing interest in recent decades because they can finely tune the catalytic properties of metals. However, there are a lot of problems that still need to be solved. Reaction induced inactive CuPd alloy inhibits the reduction of highly active Cu_2O for $CuPd–Cu_2O/Ti$ powder, but the conversion is lower than 90% at the temperature of 280 °C.[4] The synergistic effect between Au and Pd species in $AuPd/TiO_2$ is prominent in the oxidation of alcohols compared with Au/TiO_2 or Pd/TiO_2, but the tedious preparation process and the low efficiency impede its applications.[10,11]

Based on the problems mentioned above, the major challenge is to develop an effective catalyst endowed with high activity at low temperature coupled with high thermal conductivity to enhance the catalyst stability.[6] SiC powder is chosen as support because of its excellent heat conductivity, low price and high oxidation/corrosion resistance behavior.[5] The synergistic effect between Pd and oxides such as Cu_2O has been reported,[4] but the reaction temperature is still high and the reaction induced process (the alcohol could convert inactive fresh catalyst into active catalyst) has not been discussed. As a continuation of our previous research, *in situ* reaction-induced Pd_3Bi_5/SiC catalyst is prepared by a simple impregnation and calcination method. The transformation from $PdO–Bi_2O_3$ to $Pd^0–Bi_2O_3$ is confirmed, which is testified by XRD and XPS. The synergism between Pd and Bi_2O_3 is prominent due to excellent catalytic activity of PdBi/SiC and the inferior catalytic activities of Pd/SiC or Bi/SiC.

2. Experimental section

2.1 Materials and methods

SiC powder (200–300 mesh with surface area of 0.15 $m^2\ g^{-1}$), $Pd(NO_3)_2\cdot 2H_2O$ and $Bi(NO_3)_3\cdot 5H_2O$ were purchased from Sinopharm Chemical Reagent Co Ltd. SBA-15 and MCM-41 were supplied by Nankai University Catalyst Co Ltd. Other substrates were supplied by Aladdin Reagent Co. Ltd.

All catalysts were characterized by inductively coupled plasma atomic emission spectrometry (ICP-AES, ICP Thermo

---

Research Center of Resource Recycling Science and Engineering, College of Arts and Sciences, Shanghai Polytechnic University, Shanghai 201209, China. E-mail: pwwang@sspu.edu.cn; wangjifen@sspu.edu.cn

† Electronic supplementary information (ESI) available. See DOI: 10.1039/d0ra07859j

IRIS Intrepid II XSP; USA), X-ray photoelectron spectroscopy (XPS, Escalab 250xi spectrometer, Al Kα, adventitious C 1s line (284.8 eV) as the reference), X-ray diffraction (XRD, Rigaku Uitima IV diffractometer with Cu Kα radiation (35 kV and 25 mA); Japan), scanning electron microscopy (SEM, Hitachi S-4800; Japan) equipped with an energy dispersive X-ray fluorescence spectrometer (EDX, Oxford; UK), O_2-temperature programmed desorption (O_2-TPD) measurements were performed on a Quanta chrome ChemBET 3000 (USA) chemisorption apparatus with a thermal conductivity detector (TCD), and transmission electron microscopy (TEM, FEI-Tecnai G2 F30; USA). ^{1}H NMR spectra were recorded on a Bruker 400 or a Agilent 400 (100 MHz).

2.2 Preparation of the catalysts

Pd_3Bi_5/SiC fresh (weight loading of Pd and Bi was 3 wt% and 5 wt% respectively) was prepared by impregnation of 1 g SiC powder, 65 mg $Pd(NO_3)_2 \cdot 2H_2O$, 116 mg $Bi(NO_3)_3 \cdot 5H_2O$ and 2 mL H_2O followed by being dried at 100 °C overnight and calcinated at 300 °C in air for 2 h, which was denoted as Pd_3Bi_5/SiC fresh. Additionally, other catalysts such as Pd_xBi_y/SiC fresh, Pd_x/SiC fresh and Bi_y/SiC fresh (x and y indicate the weight content of Pd and Bi respectively) were prepared following the same procedure by simply tuning the weight of $Pd(NO_3)_2 \cdot 2H_2O$ or $Bi(NO_3)_3 \cdot 5H_2O$. The fresh catalysts (Pd_xBi_y/SiC fresh, Pd_x/SiC fresh and Bi_y/SiC fresh) after 1 h running (Time on steam (TOS) of 1 h) in the reaction conditions (see Section 2.3, catalytic tests) were denoted as Pd_xBi_y/SiC, Pd_x/SiC and Bi_y/SiC for short.

2.3 Catalytic tests

The gas phase selective oxidation process was carried out on a fixed-bed reactor (inner diameter of 10 mm) under atmospheric pressure made up by ourselves (Scheme S1†). Catalyst used in each experiment was 0.3 g (200–300 mesh) and alcohols are fed continuously by a peristaltic pump, in parallel with O_2 (oxidant) and N_2 (dilute gas) feeding using the calibrated mass flow controllers, into the reactor heated to 240 °C. WHSV (weight hourly space velocity) of alcohol was 20 h^{-1} and the molecular ratio of alcohol/O_2/N_2 is 1/0.6/2.4. The products were analysed by Gas Chromatography (SP-7820 with TCD detector). The calculation method of benzyl alcohol conversion and benzaldehyde selectivity were listed in the ESI.† All the catalytic tests were repeated for 3 times to improve accuracy.

In order to prevent the oxidation of our catalysts after reaction, the spent catalysts are collected until cooling down to room temperature under the protection of N_2.

3. Results and discussion

3.1 Catalytic activity

The catalytic activities of the catalysts are shown in Table 1. Given the strong exothermic effect in the gas phase oxidation of alcohol, the chemically inert SiC powder with excellent thermal conductivity and high oxidation resistance behaviour other than oxides (such as Al_2O_3 and TiO_2) or zeolites (such as SBA-15) is selected as supports (Table 1, entry 1). The catalytic behaviour of pure Pd_x/SiC catalysts is very low (Table 1, entries 2 and 3), which is in accordance with previously reported Pd/Ti powder catalyst.[4] It is noted that Bi_y/SiC catalyst is nearly inactive in alcohol oxidation even with Bi content increasing to 5% (Table 1, entries 4 and 5). At 280 °C, the conversion of benzyl alcohol increases from 90% to 95% with Pd loading increasing from 1% to 2% (Table 1, entries 6 and 8) for Pd_xBi_5/SiC catalyst, which is nearly unchanged with Pd loading further increasing to 3% (Table 1, entry 10). As for Pd_xBi_5/SiC catalysts, further increasing the Pd content to 4% or 5% does not yield better performance (Table 1, entries 16 and 17), indicating that there may be

Table 1 Catalytic activity of the catalysts[a]

Entry	Catalyst	Content of Pd[d] (wt%)	Content of Bi[d] (wt%)	Conversion[e] (%)	Selectivity[f] (%)
1	SiC	0	0	3	97
2	Pd_1/SiC	0.96	0	11	98
3	Pd_5/SiC	4.68	0	31	99
4	Bi_1/SiC	0	0.88	2	98
5	Bi_5/SiC	0	4.70	6	97
6	Pd_1Bi_5/SiC	0.90	4.68	90	97
7[b]	Pd_1Bi_5/SiC	0.90	4.68	78	98
8	Pd_2Bi_5/SiC	1.82	4.81	95	98
9[b]	Pd_2Bi_5/SiC	1.82	4.81	88	98
10	Pd_3Bi_5/SiC	2.90	4.52	98	97
11[b]	Pd_3Bi_5/SiC	2.90	4.52	93	98
12[c]	Pd_3/SiC&Bi_5/SiC	2.71	4.83	25	97
13[b]	CuPd–Cu_2O/Ti	3.10	0	65	99
14	Pd/TiO_2	0.7	0	50	98
15	Pd/SBA-15	1.0	0	99	99
16	Pd_4Bi_5/SiC	3.8	4.89	97	95
17	Pd_5Bi_5/SiC	4.9	4.92	97	96

[a] Reaction conditions: catalyst 300 mg, temperature 280 °C, O_2/alcohol/N_2 = 0.6/1/2.4 and WHSV 20 h^{-1}. [b] Temperature 240 °C. [c] Pd_3/SiC and Bi_5/SiC are physically mixed. [d] The content is confirmed by ICP. [e] Conversion of benzyl alcohol. [f] Selectivity of benzaldehyde.

Table 2 Influence of supports[a]

Catalyst	ΔT^b (°C)	Conversion[c] (%)	Conversion[d] (%)
Pd_3Bi_5/SiC	6	98	90
Pd_3Bi_5/Al_2O_3	32	93	68
Pd_3Bi_5/TiO_2	25	96	75
Pd_3Bi_5/SiO_2	36	93	65
Pd_3Bi_5/SBA-15	30	95	72

[a] Reaction conditions: catalyst 300 mg, temperature 240 °C, O_2/alcohol/N_2 = 0.6/1/2.4 and WHSV 20 h^{-1}. [b] ΔT is the temperature difference between catalyst bed and reactor external wall. [c] Conversion of benzyl alcohol after 2 h running. [d] Conversion of benzyl alcohol after 20 h running.

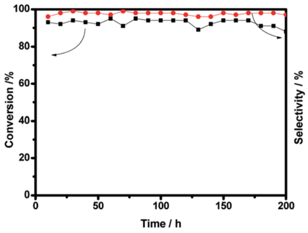

Fig. 1 Long-term test for the Pd_3Bi_5/SiC catalyst.

sufficient Pd^0–Bi_2O_3 interface in the reaction. So Pd_3Bi_5/SiC is selected as the optimal catalyst given to its excellent catalytic activity and thermal conductivity, which exhibits remarkable performance compared with previously reported Pd based catalysts. However, the catalytic activity of Pd_3Bi_5/SiC is much higher than that of Pd_1Bi_5/SiC and Pd_2Bi_5/SiC at the lower temperature of 240 °C (Table 1, entries 7, 9 and 11).

Interestingly, the conversion of benzyl alcohol is just 25% when Pd_3/SiC and Bi_5/SiC are physically mixed (Table 1, entry 12), which is similar to the previously reported $Ag_{2.5}Cu_5$/SiC catalyst.[6] So Pd_3Bi_5/SiC exhibits excellent heat conductivity in the low temperature gas phase oxidation of alcohols. Furthermore, the influence of support in this reaction could be neglected (Table 2). Thus Pd_3Bi_5/SiC is selected as the optimal catalyst given its excellent catalytic activity and thermal conductivity, which exhibits remarkable performance compared with previously reported Pd based catalysts. Anti-sintered large size Pd particles show inferior catalytic activity compared with aforementioned catalysts (Table 1, entry 14).[3] For benzyl alcohol oxidation at 240 °C, Pd_3Bi_5/SiC delivers a single run life time of 200 hours with excellent activity and selectivity (Fig. 1). For aromatic alcohols, such as 1-phenylethanol and 2-phenylethanol, the conversion is 75% and 55% respectively and the selectivity of phenylacetaldehyde and acetophenone is 98% and 97% respectively. For methanol and ethanol, the conversion is 91% and 88% respectively (Table S1†).

3.2 Physicochemical characterization of fresh Pd_3Bi_5/SiC catalyst

In order to further identify the active site in the reaction, Pd_3Bi_5/SiC fresh is characterized elaborately by XRD and XPS because valance effect other than particle size or surface area plays an important role in the gas phase oxidation of alcohols.[12,13] XRD and XPS indicate that PdO and Bi_2O_3 are formed after calcination of nitrate salts with SiC powder. Given the weak characteristic diffraction peaks of PdO centered at $2\theta = 31.5°$ (Fig. 2A), we conclude that the particle size is very small, which is in accordance with the previous report.[7] Just like PdO nanoparticles, the small size Bi_2O_3 nanoparticles are formed given the weak characteristic diffraction peak centered at $2\theta = 27.4°$ (Fig. 2A). Pd 2p spectrum indicates that the binding energy peak at 336.6 eV is assigned to PdO[2,3,8] (Fig. 2B). The binding energy of Bi is centered at 160.0 eV, which is much higher than that of metallic Bi (Fig. 2C).[14,15] Hence, the electron transfer from Bi to O is prominent and Bi_2O_3 is formed in the pre-treatment conditions. Just like Pd_3Bi_5/SiC fresh, PdO and Bi_2O_3 are formed for Pd_3/SiC fresh and Bi_5/SiC fresh respectively (Fig. 2A).

3.3 Formation of active site and the influence of supports

Compared with Pd_3/SiC and Bi_5/SiC, reaction induced Pd^0–Bi_2O_3 species from PdO–Bi_2O_3 in the reaction conditions plays an important role in the catalytic activity (Table 1, entries 3, 5 and 11), which is verified by XRD, TEM and XPS. XRD pattern indicates that the diffraction peak of Bi_2O_3 remains unchanged while the diffraction peak of PdO disappears and the new diffraction peaks of Pd form compared with Pd_3Bi_5/SiC fresh

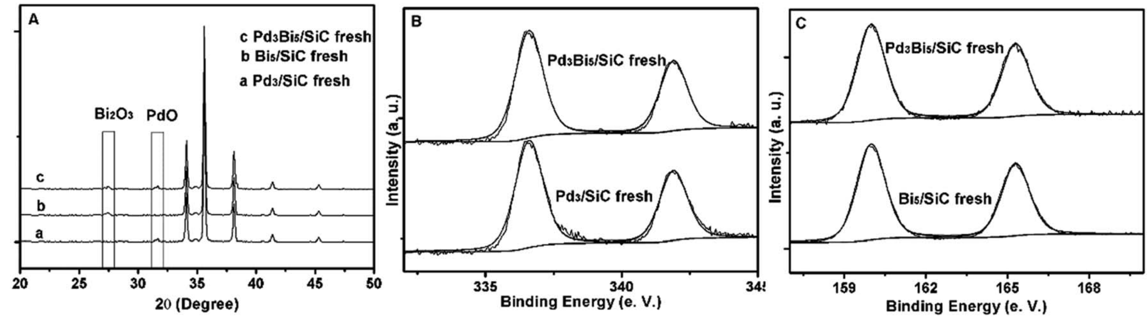

Fig. 2 (A) XRD patterns of the Pd_3/SiC fresh, Bi_5/SiC fresh and Pd_3Bi_5/SiC fresh; (B) Pd 2p spectrums of Pd_3/SiC fresh and Pd_3Bi_5/SiC fresh; (C) Bi 2p spectrums of Bi_5/SiC fresh and Pd_3Bi_5/SiC fresh.

(Fig. 3A). Pd 2p spectrum indicates that the strong binding energy peak at 335.3 eV is prominent, so Pd^0 is formed in the reaction conditions (Fig. 3B).[3,4] The binding energy of Bi 2p is close to that of the fresh catalyst, so XRD and XPS indicate that Bi_2O_3 remains unchanged in the reaction conditions (Fig. 3C). TEM indicates that the ensembles consist of the small size 5.8 nm Pd^0 or Bi_2O_3 nanoparticles (Fig. 3D). The lattice fringes of Pd nanoparticle and Bi_2O_3 nanoparticle are 0.225 nm and 0.326 nm respectively, which is in accordance with XRD results and the previous reports (Fig. 3E and F).[4,14,15] The mapping images indicate that Pd, Bi and O distribute on the support randomly and the agglomeration of the nanoparticles is inhibited after the reaction conditions (Fig. 3G–I). Furthermore, TEM images show that the particle sizes of used Pd_3/SiC and Bi_5/SiC catalysts are 5.5 and 6.5 nm respectively, so the influence of particle size effect on the catalytic activity could be excluded (Fig. S1†). Moreover, TG curve shows that the carbon content is lower than 2 wt%, showing the excellent thermal conductivity of SiC powder (Fig. S1†). In order to further testify the active phase in the oxidation of benzyl alcohol, other supports such as Al_2O_3, TiO_2, SBA-15, SiO_2 and MCM-41 are used to prepare the catalysts. Interestingly, Pd_3Bi_5/Al_2O_3, Pd_3Bi_5/TiO_2, Pd_3Bi_5/SiO_2, Pd_3Bi_5/SBA-15 and Pd_3Bi_5/MCM-41 all exhibit excellent catalytic activities in the first 2 h running (Table 2). However, the conversion of benzyl alcohol decreases rapidly after 20 h running in the reaction conditions. The catalyst bed packed with Pd_3Bi_5/SiC delivers a low ΔT (the temperature difference between catalyst bed and reactor external wall) of 6 °C at 240 °C, which is much lower than that of other catalysts (Table 2). So Pd_3Bi_5/SiC exhibits excellent heat conductivity in the low temperature gas phase oxidation of alcohols, which helps in rapidly dissipating the great quantity of reaction heat liberated from such strongly exothermic process and the influence of supports is ruled out for the oxidation of alcohols.[13]

3.4 Further discussions of active Pd^0–Bi_2O_3 and inactive PdO–Bi_2O_3 phase

For the fresh and used Pd_3Bi_5/SiC catalyst, XRD and XPS results indicate that PdO–Bi_2O_3 and Pd^0–Bi_2O_3 ensembles are the main

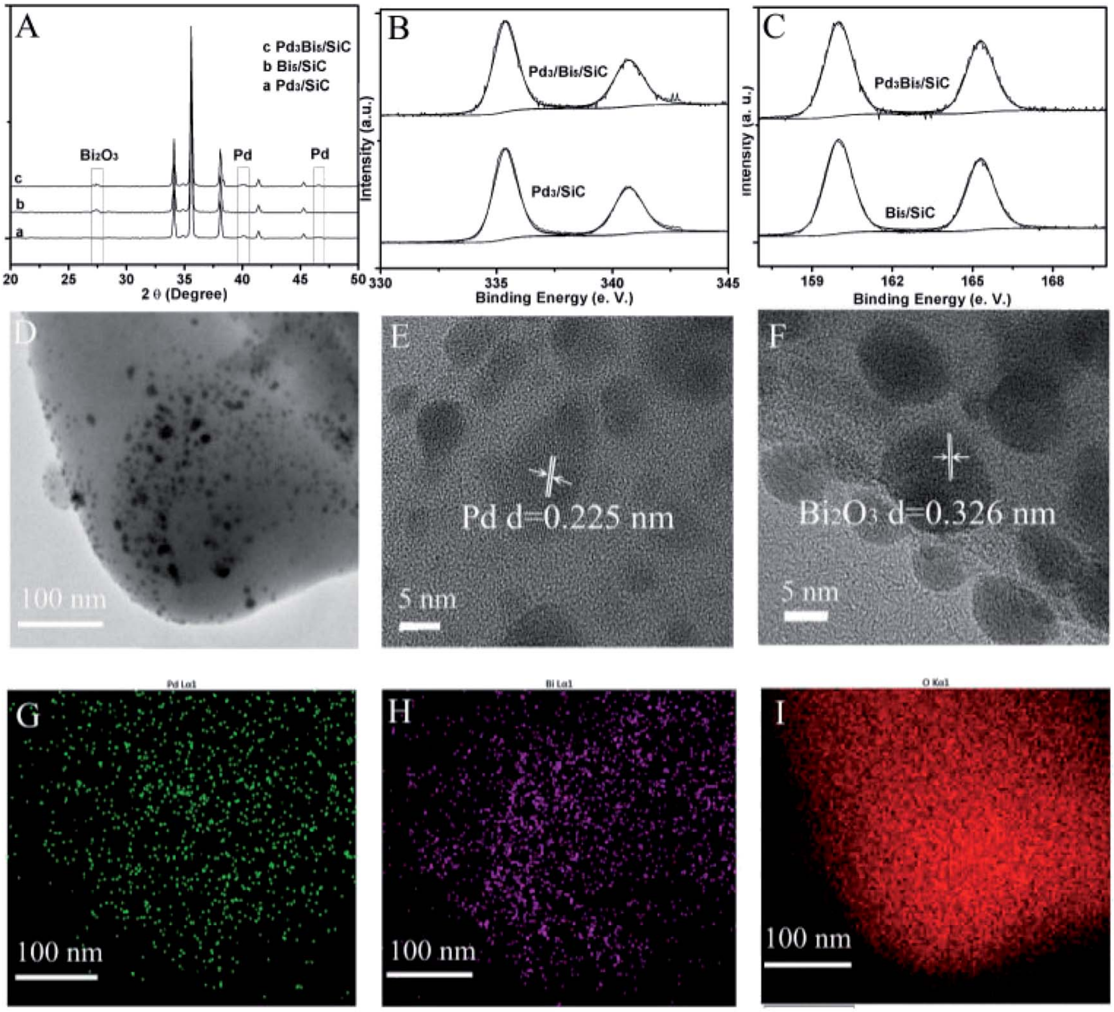

Fig. 3 (A) XRD patterns of the Pd_3/SiC, Bi_5/SiC and Pd_3Bi_5/SiC; (B) Pd 2p spectrums of Pd_3/SiC and Pd_3Bi_5/SiC; (C) Bi 2p spectrums of Bi_5/SiC and Pd_3Bi_5/SiC; (D) TEM image of Pd_3Bi_5/SiC; (E) lattice fringe of Pd in Pd_3Bi_5/SiC; (F) lattice fringe of Bi_2O_3 in Pd_3Bi_5/SiC; (E–G) distributions of Pd, Bi and O in Pd_3Bi_5/SiC.

phase in the catalyst (Section 3.2 and 3.3). Hence, reductive alcohol reduces inactive PdO–Bi_2O_3 to active Pd^0–Bi_2O_3. To further compare between the catalytic efficiency of PdO–Bi_2O_3 and Pd^0–Bi_2O_3, we compare the catalytic activities of the catalysts in the reaction conditions after different time on steam (TOS).[16] XPS results shows that the binding energy peaks at 335.0 and 336.4 eV are attributed to Pd^0 and PdO respectively (Fig. 4A). After calcinations at 300 °C, Pd species for Pd_3Bi_5/SiC exists in the form of PdO phase (Fig. 2A). The conversion of alcohol increases and the ratio of Pd^0/PdO increases with the prolongation of TOS. For example, after 10 minutes running in the reaction conditions, Pd^0/PdO ratio is 52% and the conversion of alcohol is 63% (Fig. 4A).[4] Similarly, Pd^0/PdO ratio is 73% and the conversion of alcohol is 78% after 20 minutes running in the reaction conditions (Fig. 4A).

Interestingly, PdO disappears and Pd is dominant for Pd_3Bi_5/SiC (TOS of 1 h) (Fig. 3A). XRD results show that the diffraction peak of PdO decreases and the diffraction peaks of Pd^0 increase with the prolongation of reaction time, which is corresponding with XPS results (Fig. 4B). Interestingly, it can been seen that the conversion of benzyl alcohol increases linearly with the Pd^0/PdO ratio (Fig. 4C). The diffraction peaks of support and Bi_2O_3 remain unchanged (Fig. 4B). However, given the low catalytic activity of Pd_3/SiC and Bi_5/SiC, Pd^0 or Bi_2O_3 is inactive in alcohol oxidation (Table 1, entries 3 and 5, Fig. 3A). Hence, XRD and XPS indicate that benzyl alcohol reduces the inactive PdO–Bi_2O_3 to active Pd^0–Bi_2O_3, which plays an important role in the low temperature gas phase oxidation of alcohols.

3.5 Synergistic effect between Pd and Bi_2O_3

Lots of techniques should be adopted to investigate the synergistic effect between Pd and Bi_2O_3. Reportedly, for the gas phase alcohol oxidation reaction, catalytic and oxidative dehydration are the main routes. For the catalytic dehydrogenation mechanism, the H atom in the alcohol will be captured by the oxides, which will be moved by oxygen with the aid of metals. However, for the oxidative dehydrogenation mechanism, active oxygen species will be participated into the Mars Krevelen mechanism.[17,18]

The chemical absorbed oxygen couldn't be detected by O_2-TPD and the conversion of alcohol will be about 5–10% in the absence of O_2 for the catalytic dehydrogenation system. However, the chemical absorbed oxygen could be detected by O_2-TPD and the conversion of alcohol will be about 1–2% in the absence of O_2 for the oxidative dehydrogenation system. Hence, absorbed oxygen species plays an important role in the oxidative dehydrogenation other than catalytic dehydrogenation.[17,18]

To differentiate the two mechanisms over Pd_3Bi_5/SiC catalyst, the control experiments in the absence of O_2 are conducted firstly. The conversions of benzyl alcohol are about 7–9% at 240 °C for Bi_5/SiC and Pd_3Bi_5/SiC. Secondly, O_2-TPD shows there are no O_2 desorption peaks on the two catalysts (Fig. S2†). So the catalytic oxidation cycle is tentatively proposed.

Just like Cu-based catalysts, to further confirm the catalytic oxidation cycle, solid state ^1H NMR is used to characterize the Bi_2O_3–H species. Four catalysts, Pd_3Bi_5/SiC (a), Pd_3Bi_5/SiC reacted with benzyl alcohol in the absence of O_2 at 240 °C for 2 h (b), Bi_5/SiC (c), Bi_5/SiC reacted with benzyl alcohol in the absence of O_2 at 240 °C for 2 h (d) are used to probe the Bi_2O_3–H species. The ^1H NMR signal at 1.3 and 4.9 pm are corresponding with Bi_2O_3–H and H_2O (Fig. 5). For the catalysts (b) and (d), the similar strong hydride HNMR peaks are obtained, showing their similar catalytic dehydrogenation activity. However, the Bi_2O_3–H signal decreases obviously on Pd_3Bi_5/SiC ($A_a/A_b = 0.30$), while decreases slightly over Bi_5/SiC ($A_a/A_b = 0.82$).

In the end, the TOF values of Pd_3Bi_5/SiC and Pd_3/SiC are calculated (Table S2†). In the experiments, the WHSVs are optimized to obtain the low benzyl alcohol conversion. The TOF values of Pd_3Bi_5/SiC is 8842 and 2210 h^{-1} at 260 and 240 °C respectively, which are about 43 and 34 times of that of Pd_3/SiC. So the results mentioned above testify that Pd^0–Bi_2O_3 is beneficial to eliminating the Bi_2O_3–H intermediates.

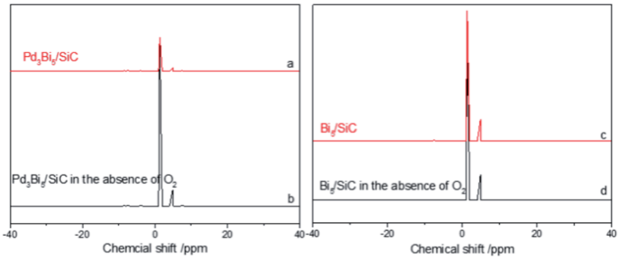

Fig. 5 H NMR spectrums of the catalysts.

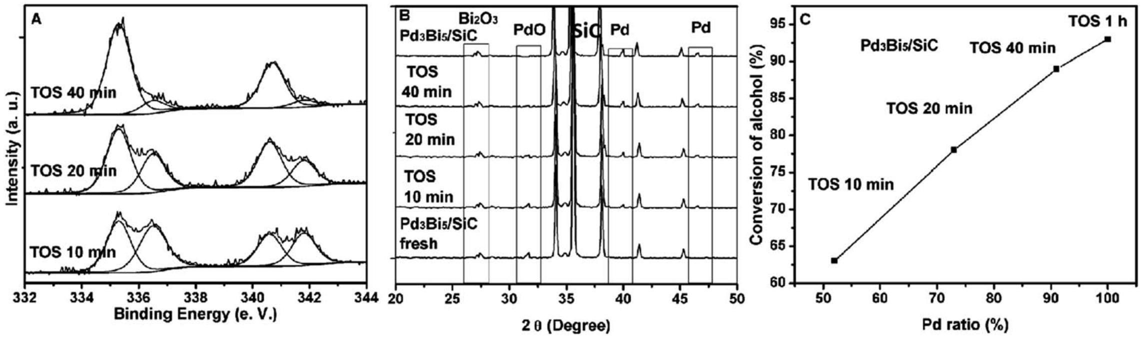

Fig. 4 (A) Pd 2p spectrums of Pd_3Bi_5/SiC (TOS of 10, 20 and 40 minutes); (B) XRD patterns of Pd_3Bi_5/SiC (TOS of 10, 20 and 40 minutes); (C) catalytic activity of Pd_3Bi_5/SiC (TOS of 10, 20 and 40 minutes).

4. Conclusions

Pd_3Bi_5/SiC was successfully prepared in a simple impregnation method, which shows excellent activity and stability in alcohol oxidation reaction. In the reaction conditions, benzyl alcohol reduces the inactive PdO–Bi_2O_3 to active Pd^0–Bi_2O_3, which plays an important role in the low temperature gas phase oxidation of alcohols. XRD, XPS and control experiments indicate that Pd^0/PdO ratio was vital for this reaction. Control experiments, O_2-TPD and ^{1}H NMR testify that Pd^0–Bi_2O_3 is beneficial to eliminating the Bi_2O_3–H intermediates.

Conflicts of interest

There are no conflicts to declare.

Acknowledgements

This work is supported by the National Science Foundation of China (Grant No. 21902100 and 51776116) and the Youth Foundation of Shanghai Polytechnic University (Grant No. EGD19XQD18). We are also grateful for the financial support from the Gaoyuan Discipline of Shanghai – Environmental Science and Engineering (Resource Recycling Science and Engineering).

References

1 P. Wu, Y. Cao, L. Zhao, Y. Wang, Z. He, W. Xing, P. Bai, S. Minova and Z. Yan, *J. Catal.*, 2019, **375**, 32.

2 N. N. Opmbe, C. Guild, C. Kingondu, N. C. Nelson, I. I. Slowing and S. L. Suib, *Int. J. Chem. Eng. Res.*, 2014, **53**, 19044.

3 K. Liu, X. J. Yan and L. Y. Dai, *Catal. Commun.*, 2015, **58**, 132.

4 K. Mori, T. Hara, T. Mizugaki, K. Ebitani and K. Kaneda, *J. Am. Chem. Soc.*, 2004, **126**, 10657–10666.

5 K. Liu, H. K. Long and J. Dong, *RSC Adv.*, 2017, **7**, 54861.

6 L. Zhao, L. P. Kong and L. Y. Dai, *Catal. Commun.*, 2017, **10**, 1.

7 C. H. Liu, C. Y. Lin and J. M. Chen, *J. Catal.*, 2017, **350**, 21.

8 X. M. Wang, G. J. Wu and L. D. Li, *Appl. Catal., B*, 2012, **115–116**, 7.

9 G. J. Wu, X. M. Wang and L. D. Li, *Appl. Catal., B*, 2013, **136–137**, 177–185.

10 G. W. Wu, G. L. Brett and G. J. Hutchings, *Catal. Sci. Technol.*, 2016, **6**, 4749.

11 N. A. Rifai, F. Galvanin and G. J. Hutchings, *Chem. Eng. Sci.*, 2016, **149**, 129.

12 G. F. Zhao, M. M. Deng and Y. Lu, *J. Catal.*, 2013, **301**, 46.

13 G. F. Zhao, Y. K. Li and Y. Lu, *AIChE J.*, 2014, **60**, 1045.

14 H. B. Liao, J. H Zhu and Y. L. Hou, *Nanoscale*, 2014, **6**, 1049.

15 H. Xu, K. Zhang and P. Yang, *J. Power Sources*, 2017, **356**, 27.

16 P. W. Wang, G. F. Zhao and Y. Lu, *Sci. Adv.*, 2017, **3**, 1.

17 G. F. Zhao, H. Y. Hu, M. M. Deng, M. Ling and Y. Lu, *ChemCatChem*, 2011, **3**, 1629.

18 K. Liu, C. Hou, Y. B. Sun and X. Q. Cao, *Catal. Commun.*, 2020, **135**, 105892.